Continuous Localization of Cardiac Activation Sites Using a Database of Multichannel ECG Recordings

Mark Potse*, *Student Member, IEEE*, André C. Linnenbank, *Associate Member, IEEE*, Heidi A. P. Peeters, Arne SippensGroenewegen, and Cornelis A. Grimbergen, *Member, IEEE*

***Abstract*—Monomorphic ventricular tachycardia and ventricular extrasystoles have a specific exit site that can be localized using the multichannel surface electrocardiogram (ECG) and a database of paced ECG recordings. An algorithm is presented that improves on previous methods by providing a continuous estimate of the coordinates of the exit site instead of selecting one out of 25 predetermined segments. The accuracy improvement is greatest, and most useful, when adjacent pacing sites in individual patients are localized relative to each other. Important advantages of the new method are the objectivity and reproducibility of the localization results.**

***Index Terms*—Body surface mapping, electrocardiography, pace mapping, ventricular tachycardia.**

I. Introduction

ELECTROCARDIOGRAPHIC body surface mapping is used in the catheterization laboratory to perform high resolution localization of endocardial exit sites of ectopic ventricular beats and monomorphic ventricular tachycardia (VT) [1]–[4]. For this purpose, the surface potentials during such an arrhythmia are summed over the QRS interval of the electrocardiogram (ECG). Using the resulting *QRS integral map* (QRSI), the exit site can be localized to one of 25 different segments of origin in the structurally normal human left ventricle [1]. The latter result is obtained using a database consisting of 25 mean paced QRSI's [1] (see Fig. 1). Each mean QRSI in the database corresponds to a known endocardial segment of activation onset. The exit site of a VT can be predicted by comparing its QRSI with the paced QRSI's in the database.

A three-phase mapping procedure is currently used in our group to guide the catheter to the optimal site for curative ablation [5]. First, a QRSI is obtained from the target arrhythmia.

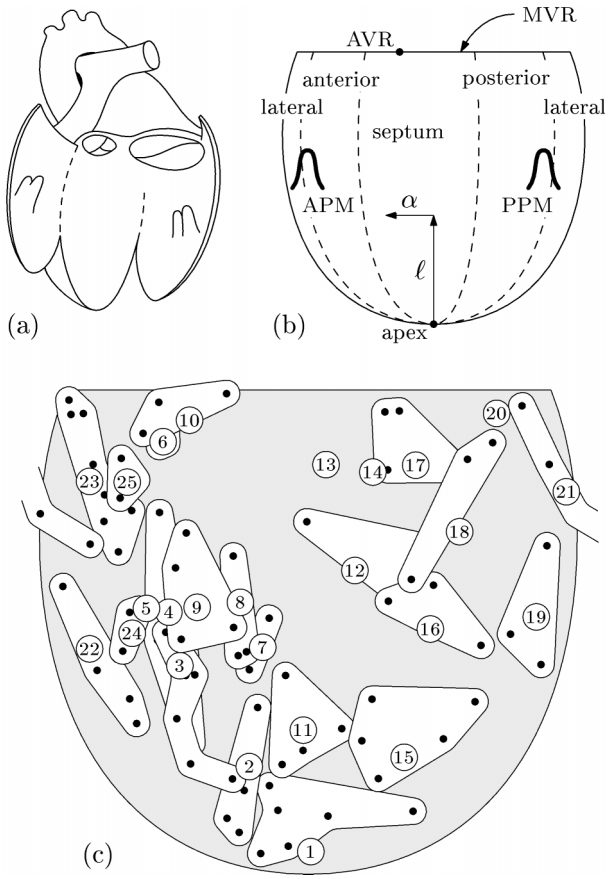

Fig. 1. (a) Cut-open view of the left ventricle and (b) illustration of the left ventricular (LV) diagram. This diagram displays the endocardium, opened at the lateral wall; it resembles the cut-open view shown in (a). The top edge represents the mitral valve ring, the apex is indicated at the bottom. The width mimics the circumference of the ventricle as a function of the ventricular length. Also indicated are the four longitudinal quadrants (anterior, septum, posterior, and lateral) separated by dashed lines, the anterior and posterior papillary muscles (APM and PPM) and the aortic valve ring (AVR). This diagram can be generated directly from endocardial cylinder coordinates (discussed in text): ventricular length ℓ translates to the vertical distance to the apex, and the horizontal position is a fraction $\alpha/2\pi$ of the diagram width at the given length ($-\pi \leq \alpha \leq \pi$), where α represents the ventricular angle. (c) Pacing sites, indicated with dots, and pacing segments, indicated with white patches, of the database of 25 mean pace maps for the structurally normal left ventricle, created by SippensGroenewegen *et al.* [1]. Mean positions of segments are labeled with encircled numbers. Segment 21 crosses the border of the diagram.

This QRSI is displayed and compared to the database of 25 mean maps to select the best matching database map. The segment that corresponds to this database map is the initial estimate for the exit site of the arrhythmia. Maps are compared using the correlation coefficient [6].

Manuscript received September 11, 1998; revised November 24, 1999. This work was supported in part by the Dutch Technology Foundation STW under Grant AGN 66 4098. *Asterisk indicates corresponding author*.

*M. Potse is with the Medical Physics Department, Academic Medical Center, University of Amsterdam, P.O. Box 22700, 1100 DE Amsterdam, The Netherlands (e-mail: M.Potse@amc.uva.nl).

A. C. Linnenbank is with the Medical Physics Department, Academic Medical Center, University of Amsterdam, 1100 DE Amsterdam, The Netherlands.

H. A. P. Peeters is with the Section of Clinical Electrophysiology, Heart-Lung Institute, University Hospital of Utrecht, Utrecht, The Netherlands.

A. SippensGroenewegen is with the Section of Cardiac Electrophysiology, Department of Medicine, and the Cardiovascular Research Institute, University of California at San Francisco, San Francisco, CA 94143 USA.

C. A. Grimbergen is with the Medical Physics Department, Academic Medical Center, University of Amsterdam, 1100 DE Amsterdam, The Netherlands. He is also with the Control Department, Faculty of Design, Construction, and Production, Delft University of Technology, Delft, The Netherlands.

Publisher Item Identifier S 0018-9294(00)03286-9.

Second, an endocardial catheter is positioned at the identified ventricular segment. By electrical stimulation with the distal electrode pair of the catheter, ectopic heart beats are electrically induced (paced) while the position of the catheter tip is monitored using biplane X-ray imaging. The surface electrocardiogram corresponding to the paced beats is recorded, and the QRSI of a paced beat is computed. This paced QRSI is displayed and compared to the QRSI of the arrhythmia, and to the database maps, to estimate the exit site of the arrhythmia relative to the catheter position. The catheter is subsequently moved to the indicated site where a new paced QRSI is made. These steps are repeated until the site is found where the paced QRSI matches best with the QRSI of the arrhythmia.

In the third phase of the mapping procedure, local activation sequence mapping [7] is performed, starting at the site identified in the second phase. This procedure is aimed at finding the site where the earliest ventricular activation (premature depolarization) can be recorded, i.e., the site of origin of the arrhythmia. This is the target site for ablation, and may differ from the exit site that is found in the second phase of the procedure. Ablation is performed by applying radiofrequency current from the tip electrode of the catheter.

A limitation of the database lookup method is that it provides discrete results; the localization result of the first phase is a selection of one out of 25 possible segments of origin. This means that the estimated position cannot be more precise than the size of a segment. The segment size in this database is 3.3 ± 1.4 cm^2 [1]. In contrast, the resolution of stimulus site separation using body surface potentials has been estimated at 2–5 mm [8], [9], i.e., identification of a circular area smaller than 0.1–0.8 cm^2. The large difference between this accuracy and the mean database segment size suggests that the current method may not take optimal advantage of the attainable resolution. Another limitation of the current method is that, in the second phase, physicians have to interpolate mentally between a pace map and at least three database maps to determine the optimal site to place the catheter next; a task for which a computer program might be more adequate. A computer program would be able to make full use of the precision of body surface mapping and would provide objective and reproducible results.

The method that will be described here serves to remove the limitations that the discreteness of the database imposes, and provides objective results by giving a continuous estimate of the location corresponding to a given QRSI using the full information content of the database. The accuracy of this estimate remains of course limited by the accuracy of the database locations, and their corresponding QRSI's. However, the better resolution and the use that is made of all the information that is contained in the database—instead of just the single map that correlates best—may improve the localization accuracy considerably. More importantly, if two or more paced QRSI's are obtained from the same patient in a single session, as is the case in the second phase of the mapping procedure, a precise estimate of their relative positions is provided that can be used to guide the catheter quickly to the exit site.

A. Rationale

Paced QRSI patterns originating from the left ventricle are mainly determined by the pacing position on the endocardial surface of the left ventricle [1], [10]. If we assume that the activation sequence is uniquely determined by the pacing site and does not vary significantly from patient to patient, and if we assume that the QRSI varies continuously with the endocardial position of origin, then there exists a subspace S in the multidimensional QRSI-space with the same topology as the left ventricular (LV) endocardial wall, that is, a surface. Each point on S then corresponds to an endocardial position. By identifying S, we can compute the position in a two-dimensional approximation of the endocardium from a given QRSI by projecting the QRSI on S, and applying an $\mathbb{R}^2 \rightarrow \mathbb{R}^2$ function.

Because it was observed that the amplitude of a QRSI does not contain information on the site of origin [1], we assume that S is star-convex with respect to the origin of map space (i.e., a straight line from any point on S to the origin does not intersect S), and project it on a unit sphere in the first three dimensions after application of a Karhunen–Loève (KL) transform, previously determined from a large set of paced QRS integral maps. S can then be parameterized using spherical coordinates. The translation to the endocardial surface is obtained by fitting a continuous mapping function to a set of paced maps and their measured pacing positions.

II. Methods

A. Coordinates

The endocardial wall is described using "left ventricular cylinder coordinates" [1]. These coordinates are based on the line from the LV apex to the geometric middle of the mitral valve ring. The *ventricular length* ℓ is the distance of a position, projected on this axis, to the apex, and normalized to the axis length; the *ventricular angle* α is the angle of a position relative to the angle of the aortic valve ring (AVR). Fig. 1(b) illustrates these concepts.

B. Patients

To create the database of 25 mean paced maps for the structurally normal left ventricle, SippensGroenewegen *et al.* recorded 62-lead body surface electrocardiograms during LV pace mapping in a group of eight patients with normal cardiac anatomy. The three-dimensional (3-D) position of the catheter tip was determined quantitatively using digitized biplane X-ray images, with a localization error $\leq$7 mm [1], [11], [12] (circular area of 1.5 cm^2). A total of 99 pace maps was used to create the database; these pace maps are used here to fit and test our algorithm.

C. Recording

The 62 unipolar electrocardiograms were recorded with equipment that was previously described by Grimbergen and MettingVanRijn [13], [14]. The electrode positions, which included the standard precordial leads, were chosen from the 192 vertices of a regular 12×16 grid covering the chest and back of the patient [15], [16]. Onset and offset of the QRS interval, and suitable time instants for baseline correction were selected manually according to previously defined criteria [1]. A linear correction for baseline drift was applied. The QRS

integral map was computed by summing each lead over the QRS interval, and then interpolating the irregularly spaced sites to a regular 12×16 matrix by iterative discrete Laplacian minimization [17]. In the interpolation process, faulty leads were replaced by interpolated values in the same way as the nonmeasured grid points. For further analysis, we used the 192-element maps; this was done to work with a more universal electrode array; we could also have used the 62 leads with interpolated rejected leads.

D. Localization Algorithm

In this discussion, a QRSI is regarded as a 192-element vector, containing an element corresponding to each of the 12×16 grid points. A fixed KL transform, previously determined from the 99 QRSI's, was applied to each QRSI [18]: The covariance between the 192 "channels" of the maps was computed, and the eigenvectors $\vec{\psi}_i$ of the covariance matrix were determined using Matlab software. Then each QRSI $\vec{m}$ was expressed in terms of these (orthonormal) eigenvectors, as

$$\vec{m} = \sum_{i=1}^{192} w_i \vec{\psi}_i$$

where

$$w_i = \vec{m} \cdot \vec{\psi}_i. \tag{1}$$

We found that the first three coefficients w_i, which correspond to the three $\vec{\psi}_i$ with the largest eigenvalues, describe at least 90% ($97 \pm 2\%$) of the energy content of $\vec{m}$, that is, $({w_1}^2 + {w_2}^2 + {w_3}^2)/|\vec{m}| > 0.9$ for each $\vec{m}$ (see results).

The coefficients w_1, w_2, and w_3 of each map $\vec{m}$ were treated as Cartesian coordinates in a 3-D space and expressed in spherical coordinates r, θ, and ϕ, and the other 189 coefficients were discarded. The axis of the spherical coordinate system was chosen such that the database QRSI corresponding to the LV apex had $\theta = 0$. r is an estimate of the total energy content of the map, and was also discarded, because the assumption that S is star-convex with respect to the origin of map space is equivalent to the assumption that only the *pattern* of the QRSI contains information about the site of origin. If correlation coefficients are used to compare maps, the effect is also that the total energy content is discarded. The surface S, described by the θ and ϕ coordinates must now be mapped to the LV endocardial surface.

A position on the LV wall is denoted with a pair (ℓ, α), where ℓ stands for the ventricular length and α represents the ventricular angle [1] [see Fig. 1(b)]. Estimated coordinates are indicated as $\hat{\ell}$ and $\hat{\alpha}$.

We observed that the parameter θ of a QRSI corresponded approximately to the ventricular length ℓ of the site of origin, and ϕ corresponded approximately to the ventricular angle α. This is partly a result of our definition that $\theta = 0$ in the apex. The relationship between the pairs (θ, ϕ) and (ℓ, α) is illustrated in Figs. 2 and 3.

Fig. 2 shows that the relation between α and ϕ is almost linear and can be approximated by superposing a small sine wave on a straight line. Fig. 3 shows that ℓ depends primarily on θ, with a small contribution of ϕ, that can be approximated by adding

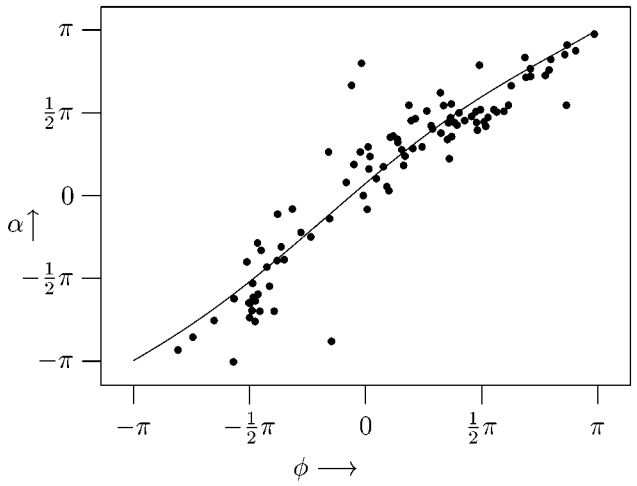

Fig. 2. Measured coordinate α of the database of 99 paced maps shown with dots versus the map coordinate ϕ. The solid line represents the estimate $\hat{\alpha}$ computed with (2).

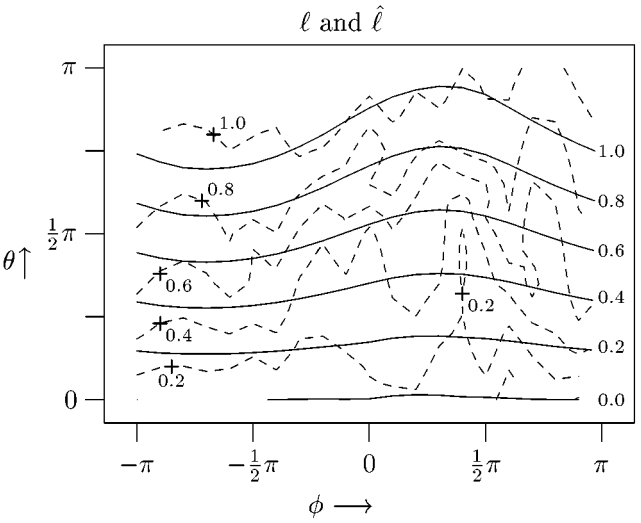

Fig. 3. Measured coordinate ℓ of the 99 paced maps, interpolated in the θ–ϕ plane, shown with dashed contour lines; these contour lines are labeled with "plus" signs. Also shown, with solid contour lines, labeled on the right side of the plot, is the estimate $\hat{\ell}$ computed with (3) (see text for details).

a sine wave contribution that is slightly larger for higher values of θ. We devised the following functions to relate ℓ and α to θ and ϕ:

$$\hat{\alpha} = \phi + c_1 + c_2 \sin(\phi - c_3) \tag{2}$$

$$\hat{\ell} = \theta\big(d_1 + d_2 \sin(\phi - d_3)\big)/\pi. \tag{3}$$

The parameters c_i and d_i of functions (2) and (3) are obtained by fitting these functions to the database maps. The resulting functions $\hat{\alpha}$ and $\hat{\ell}$ are shown by solid lines in Figs. 2 and 3, respectively.

E. Relative Localization

The primary purpose of the algorithm is to provide catheter displacement advise. For that purpose it must estimate the positions of pacing sites relative to each other, rather than relative to the endocardium. This kind of localization is referred to as "relative localization." The computation of the position itself will

be referred to as "absolute localization." We estimate the accuracy of relative localization by computing the difference between pairs of measured pacing sites and comparing it to the difference between the pacing sites predicted by the algorithm.

F. Error Measures

Errors in absolute and relative localization were computed by projecting the localization result, which is given in LV cylinder coordinates, on a triangulated model of the ventricular wall. The model was scaled such that the length of the axis from the apex to the geometric middle of the mitral valve ring was 85 mm. Localization differences can then be expressed as 3-D distances in millimeters, in order to provide an indication of the resolution of the algorithm.

G. Tests

Training and testing were performed using the same set of 99 pace maps. In order to obtain a representative and unbiased estimate of the error that the algorithm will make if applied to new maps, we used cross-validation on the 99 pace maps: the fitting procedure for c_i and d_i was applied to all but one of the database maps, the localization error of the omitted map was computed, and this procedure was repeated leaving out every map in turn. Because the error estimate is continuous, cross-validation is permissible in this situation [19].

Also, the number of maps used in the fitting procedure was decreased to see if this influenced the localization accuracy: for $N = 2 \cdots 98$ we created a test set of N maps by random selection without replacement, and used the remaining maps to fit the algorithm. This was repeated 200 times for each N, and mean, minimum, and maximum localization errors for each N were computed.

H. Display of Localization Results

Endocardial positions are displayed in a schematic diagram of the left ventricle (Fig. 1). This diagram can easily be related to a cut-open view of the left ventricle. Compared to the LV polar projection presented previously by SippensGroenewegen *et al.* [1], this diagram has the advantages that differences in α at different values of ℓ are easier to compare visually, and that the physicians involved consider it easier to translate to the cardiac image that they have in mind during a catheterization procedure. A drawback is that this diagram, contrary to the polar projection, is discontinuous along a line from the apex to the mitral valve ring.

III. RESULTS

A. Representation

The first step in the localization algorithm is to represent each map $\vec{m}$ with a triple of coefficients (w_1, w_2, w_3) as $\vec{m}' = w_1\vec{\psi}_1 + w_2\vec{\psi}_2 + w_3\vec{\psi}_3$. The associated representation accuracy is expressed as

$$\sum_{i=1}^{3} {w_i}^2 \Big/ \sum_{i=1}^{192} {m_i}^2 \tag{4}$$

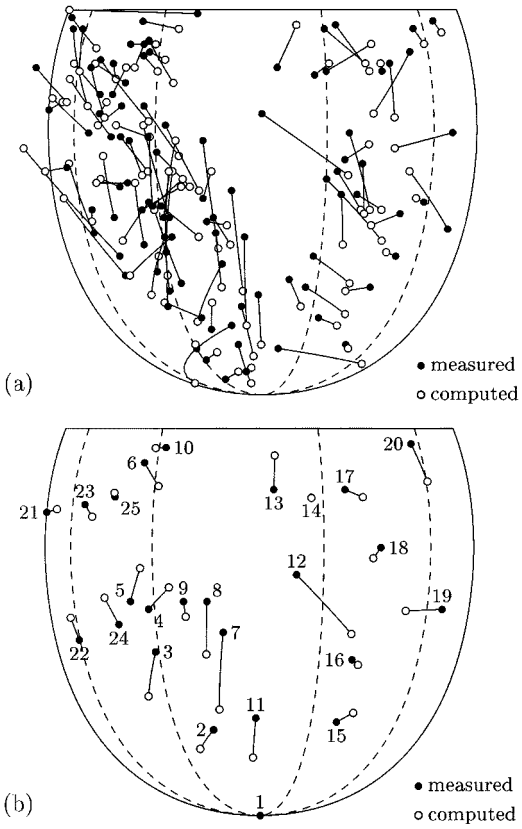

Fig. 4. (a) Differences between positions computed from the θ and ϕ coordinates of the 99 pace maps by the functions (2) and (3), and corresponding measured positions where pacing was performed. The computed positions are indicated by open circles, the measured positions by black dots. (b) Differences between the positions of the 25 database mean maps as determined by SippensGroenewegen *et al.* [1] and the corresponding computed positions of the database QRSI's.

with w_i as defined in (1). For the 99 pace maps, this number was $97 \pm 2\%$ (range 90%–99%).

B. Localization

Fig. 4 illustrates the differences between the measured and computed locations of the 99 pace maps in a schematic representation of the left ventricle. Also shown are the positions of the 25 database mean maps [1], corresponding to the 25 segments shown in Fig. 1(c).

The distance between the measured and computed positions of the 99 pace maps was 14.6 ± 8.2 mm; the distance between the 25 mean segment positions and the segment positions computed from the corresponding mean maps [1] was 9.2 ± 3.0 mm. In Fig. 5, the localization results for a subset of five pace maps, obtained in four patients, are shown. It is clear that the localization differences of maps originating in the same region were diverse in size and direction, but, as illustrated in Fig. 6, were similar if only maps of a single patient were considered.

If pairs of pace maps are considered from the same patient, with closely separated measured positions, the error for relative localization can be estimated. The mean value of this error depends on what we consider "closely separated." Therefore, we constructed several groups of pace map pairs, each group with a maximum measured distance L_g between the members of each

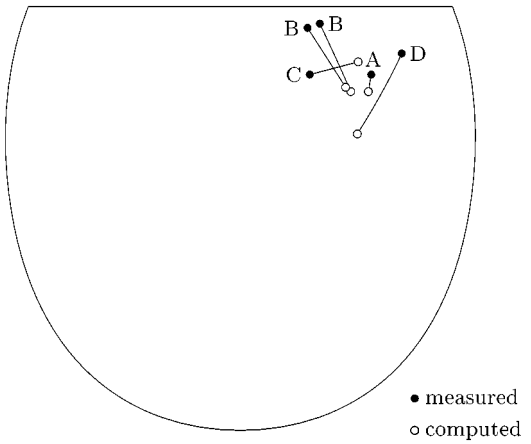

Fig. 5. Computed and measured positions corresponding to five pace maps obtained at a similar location (the basal posterolateral wall of the left ventricle) in four different patients, labeled A, B, C, and D. Black dots indicate measured positions, open circles indicate computed positions. The computed positions of all maps are close together, but the deviations from the measured positions are different in size and direction. The two maps of patient B have approximately the same error.

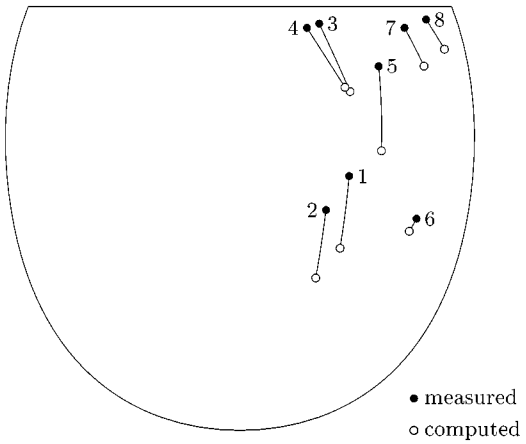

Fig. 6. Computed and measured positions corresponding to eight pace maps obtained at a similar location (the middle and basal posterolateral wall of the left ventricle) in a single patient. Considerable errors exist, but they are closely related, and the relative positions of measured and computed locations are approximately the same. Similar systematic shifts were observed in all patients.

TABLE I
LOCALIZATION ERRORS

L_g (mm)	abs. err. (mm)	rel. err (mm)	p	N_g
5	12.0±6.6	6.7±5.0	$2.4 \cdot 10^{-2}$	14
10	13.2±6.2	8.9±6.7	$3.9 \cdot 10^{-3}$	40
15	14.4±6.7	10.2±6.0	$6.8 \cdot 10^{-5}$	77
20	13.5±6.8	11.7±6.9	$3.5 \cdot 10^{-2}$	130
25	13.2±7.0	12.3±7.0	$2.3 \cdot 10^{-1}$	172
30	13.6±7.2	13.6±7.7	1.00	226

pair. We refer to the number of maps in each group as N_g; for larger L_g, more pairs can be found. Errors in relative localization were then computed for each group; results are given in Table I. Each row of the table shows errors of relative and absolute localization for all pairs in a group, as well as the significance level p for the difference between errors for absolute and relative localization in the group, and the number of pairs in the group, N_g. The significance level p was computed using Student's t-test. We found that for pairs of pace maps whose measured positions were closer than 20 mm, the error for relative localization was significantly smaller than the error for absolute localization.

Localization results obtained using reduced sets of maps for the fitting procedure, and using the remaining maps for testing, are shown in Fig. 7. This figure shows that the mean error was constant for 98 downto 20 maps, and that the maximum error increased only slightly when reducing the fitting set to approximately 40 maps.

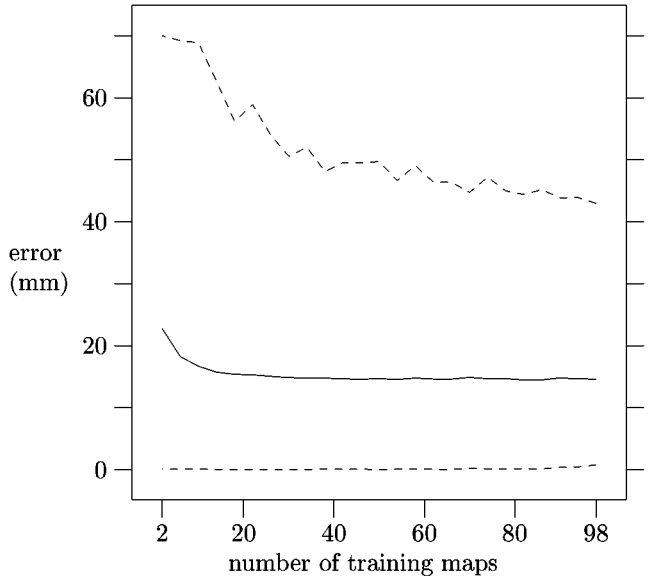

Fig. 7. Localization error for database mean maps as a function of the number of maps used for the training procedure, computed for 2 upto 98 training maps. The mean error is shown with a solid line, minimum and maximum errors are shown with dashed lines.

IV. DISCUSSION

An algorithm is proposed that can provide a continuous estimate of the site of origin of a paced QRSI. Using pace maps obtained in a specific patient, it can be used for relative localization: the assesment of *differences* in catheter positions.

For the purpose of relative localization, the algorithm depends on two assumptions: 1) the QRSI must vary continuously with the site of origin and 2) the set of all possible QRSI's that result from LV pacing must be star-convex. The first assumption is corroborated by the observation of gradually changing patterns both in measured [1] and computed [10] QRSI's. The extent to which the second assumption can be tested depends directly on the accuracy of the position measurements. For absolute localization using this algorithm, we must also assume that the relation between QRSI and site of origin is the same in all subjects. This is known to be true only in a very loose sense; this is one source of the large error for absolute localization of 14.6 ± 8.2 mm (Section III-B). Interpatient differences in thoracic anatomy, position and orientation of the heart, electrical conduction, and perhaps small differences in wavefront propagation due to varying underlying anisotropy may all contribute in causing different mappings between QRSI pattern and exit site. From the work of Hren *et al.* [20] it may be deduced that

differences in torso boundary alone may account for approximately 10 mm localization difference. These differences will be less prominent in relative localization than in absolute localization. A tailor-made database, using only pace maps from a single patient, would reduce the latter error. However, with our current data, featuring eight patients with 6–23 pace positions each, we did not obtain better results when applying the fitting and testing procedure to only the maps of a single patient. With this data, only relative localization could be shown to work as a means to adapt the method to individual patients (Table I).

Apart from nonapplicability of the assumptions, there are several possible explanations for differences between computed and measured positions:

- Errors in the X-ray localization can cause errors in the database, as well as errors in the positions that are used for evaluation. These errors can be as large as 7 mm [11], [12].
- Interpatient differences in the local geometry of the ventricular wall can cause different mappings from substrate to cylinder coordinates; these differences may be expected to be less prominent in relative localization.
- Inaccuracies in the mapping functions increase the difference between measured and computed locations. The mapping functions used to compute ventricular positions from QRSI's are simple, and somewhat arbitrary. The localization accuracy might be improved by using a better mapping function, such as a self-organizing map [21]. These differences may also be expected to be less prominent in relative localization.
- Changes in QRSI pattern with the respiratory phase may influence the localization accuracy. Amoore *et al.* [22] reported that the patterns of body surface potential maps shifted inferiorly by about 2 cm at deep inspiration. The localization algorithm is sensitive to shifting. However, pace maps were recorded in a similar respiratory phase [1], so the respiratory disturbance may be considered to play only a minor role.
- Noise and distortion of the ECG may increase the localization error.
- Data loss due to the selection of only three parameters to describe a QRSI (average accuracy $97 \pm 2\%$; range 90% to 99%) may influence the localization accuracy. However, the representation error was related to the localization error in only one of eight patients ($r = 0.63$ for 13 pace maps). Moreover, it is likely that the selection of three KL coefficients reduces noise and removes some patient-specific features of the QRSI. We observed that the KL transformation matrix, which was created from the 99 QRSI's themselves, could be replaced by others, created from potential maps of other patient groups, yielding a much larger average representation error (over 15%), with only a minor change in localization error.

Taking the most important sources of errors into account, we expect our data not to be more accurate than about 10 mm. In this respect, we believe that the 14.6 mm absolute and 10.2-mm relative accuracy (Table I, $L_g = 15$ mm) indicate that the approach is sound, and that more accurate techniques for catheter localization are necessary to establish the accuracy of our method.

For pairs of paced maps whose measured distances L_g are below 15 mm, an average localization error of 10.2 mm was obtained; for L_g under 5 mm, the average error was only 6.7 mm. This is a very small error; however, it is on average larger than the measured distance.

By reducing the number of maps used for the fitting procedure, we have shown that the number of pace maps used is high enough: the number of maps may be reduced to 20 without any impact on the average localization error; only the maximum error increases slightly. Perhaps a small decrease in maximum error may be expected if the number of pace maps would be increased beyond the current 99.

In a previous study, Muilwijk *et al.* [23] compared the results of localization by body surface mapping, using database lookup, with the results of intraoperative mapping in 62 VT morphologies obtained in 42 patients with previous anterior or inferior myocardial infarction. These authors reported a distance of 18 ± 14 mm between the exit site localized by body surface mapping and the intraoperatively determined site of origin (which may not coincide with the true exit site of the VT). The resolution reported in the present study is better, which is to be expected since we compared the computed pacing site directly to the measured pacing site.

Because there is no data available of intraoperatively determined VT *exit sites*, in combination with body surface maps of the same arrhythmia, there is no gold standard to test localization algorithms other than comparing them to the position of the catheter tip. However, catheter tip localization by biplane X-ray imaging may not be accurate enough for this purpose. Magnetic localization (using ultralow magnetic fields and a special catheter containing a miniature magnetic field sensor) [24] or electrical localization (by measuring, with the catheter electrodes, the local potential induced by small currents applied at the body surface) [25] are promising alternatives. However, the most important advantage of the described algorithm is not the improved accuracy, but rather the increased objectivity of the results, the shorter time it takes as compared to "manual" localization, and the ability to display localizations and their differences automatically. Because database interpolation is performed by a computer instead of a human observer, the results are instantly available to the computer for further processing such as automatic display of localization results in 3-D or in the standard biplane X-ray projections used in the catheterization laboratory.

The algorithm can employ different databases, for example the infarct-specific databases created by SippensGroenewegen *et al.* [2]. We expect that it can also work with delta wave maps, used by Nadeau *et al.* [26] for localization of the atrioventricular pathway in patients with the Wolff–Parkinson–White syndrome [9], [27], and to atrial databases, which contain P-wave integral maps [28].

Preliminary results indicated that the method would not work for the right ventricle. Although the technique was able to differentiate between some right ventricular (RV) paced maps, it could not differentiate between maps paced in the RV side of the septum and maps paced in the RV free wall. Such differentiation may require consideration of individual potential maps

during the QRS, or information on the amplitude of the QRSI [1] which is ignored in our current approach (i.e., for the right ventricle S is not star-convex).

An alternative for our database interpolation algorithm may be the creation of a database of any desired precision using a computer heart model, after quantitative verification of the results of this model with an empirical database. The advantage of such model studies is that they can be used with very closely separated "pacing sites," including intramural and epicardial pacing sites, and that accurate analysis of the effects of individual geometry and constitution is possible. Several groups created models that can be used for this purpose (e.g., [29] and [30]). Xu [31] and Hren [10] compared the results of such models to the database of SippensGroenewegen [1] which was also used in the present study. Their simulation results resembled those of SippensGroenewegen well, but these authors did not yet provide a quantitative evaluation of the simulation results.

The most desirable localization procedure may be provided by a computational solution of the inverse problem of electrocardiography [32], because it would, like the forward methods discussed above, provide a true understanding of the underlying electric phenomena, and in contrast to forward solutions, may be applied directly to the measured data. For example, single moving-dipole solutions for the early QRS [33], [34] or activation sequence models [35], [36] may be employed. However, these methods require excellent signal quality and accurate geometrical modeling of the subject [37], and to date no clinically practical method with sufficient accuracy has been reported. We believe that, until this kind of solution becomes available, our algorithm will provide a reasonable alternative in clinical applications.

V. Conclusion

A quantitative method is described to accurately compute the location of the endocardial site of origin of a paced body surface QRS integral map, in terms of coordinates, instead of a limited number of segments corresponding to a fixed reference set of mean paced QRSI's. Moreover, this algorithm uses information of all pace maps in the database for the localization of a single site, and leads to a continuous and regular conversion of QRSI data to LV coordinates. This is likely to improve the localization accuracy.

The most important advantages of the new method are the continuity, quantitative nature, objectivity, and reproducibility of the localization results. Also, it can be used to compute *differences* between exit- or pacing sites, thus using data measured in an individual patient to increase the accuracy.

The localization errors that were found can be attributed to a large extent to the uncertainty in the pacing position measurements. More accurate measurements may provide a better estimate of these errors.

The algorithm can be used clinically during pace mapping of LV arrhythmias to guide the catheter to the site of origin prior to ablation, and may be particularly useful due to the possibility of displaying catheter displacement advise in 3-D or in the standard X-ray projections used in the catheterization laboratory. It may also prove useful in research, for example on polymorphic ventricular tachycardia, to compute the relative positions of exit sites of consecutive beats.

Acknowledgment

The authors wish to thank Dr. H. W. Venema and Prof. Dr. A. van Oosterom for many valuable suggestions and comments.

References

[1] A. SippensGroenewegen, H. Spekhorst, N. M. van Hemel, J. H. Kingma, R. N. W. Hauer, M. J. Janse, and A. J. Dunning, "Body surface mapping of ectopic left and right ventricular activation: QRS spectrum in patients without structural heart disease," *Circulation*, vol. 82, pp. 879–896, 1990.

[2] ——, "Body surface mapping of ectopic left ventricular activation: QRS spectrum in patients with prior myocardial infarction," *Circ. Res.*, vol. 71, no. 6, pp. 1361–1378, 1992.

[3] A. SippensGroenewegen, H. Spekhorst, N. M. van Hemel, J. H. Kingma, R. N. W. Hauer, J. M. T. de Bakker, C. A. Grimbergen, M. J. Janse, and A. J. Dunning, "Localization of the site of origin of postinfarction ventricular tachycardia by endocardial pace mapping: Body surface mapping compared with the 12-lead electrocardiogram," *Circulation*, vol. 88, no. 5, pp. 2290–2306, 1993.

[4] ——, "Value of body surface mapping in localizing the site of origin of ventricular tachycardia in patients with previous myocardial infarction," *J. Amer. Coll. Cardiol.*, vol. 24, no. 7, pp. 1708–1724, 1994.

[5] H. A. P. Peeters, A. SippensGroenewegen, E. F. D. Wever, H. Ramanna, A. C. Linnenbank, M. Potse, C. A. Grimbergen, N. M. van Hemel, R. N. W. Hauer, and E. O. Robles de Medina, "Clinical application of an integrated 3-phase mapping technique for localization of the site of origin of idiopathic ventricular tachycardia," *Circulation*, vol. 99, pp. 1300–1311, Mar. 1999.

[6] A. C. Linnenbank, S. L. C. Muilwijk, A. SippensGroenewegen, and C. A. Grimbergen, "Effect of baseline procedures on QRS integral patterns in body surface maps of ventricular tachycardia," in *Proc. 13th Annu. Int. Conf. IEEE EMBS*, 1991, pp. 789–790.

[7] M. E. Josephson, L. N. Horowitz, S. R. Spielman, H. L. Waxman, and A. M. Greenspan, "Role of catheter mapping in the preoperative evaluation of ventricular tachycardia," *Amer. J. Cardiol.*, vol. 49, pp. 207–220, Jan. 1982.

[8] L. S. Green, R. L. Lux, P. R. Ershler, R. A. Freedman, F. I. Marcus, and K. Gear, "Resolution of pace mapping stimulus site separation using body surface potentials," *Circulation*, vol. 90, no. 1, pp. 462–468, July 1994.

[9] F. Molin, P. Savard, M. Dubuc, T. Kus, G. Tremblay, and R. Nadeau, "Spatial resolution and role of pacemapping during ablation of accessory pathways," *PACE*, vol. 20, pp. 683–694, Mar. 1997.

[10] R. Hren and B. M. Horáček, "Value of simulated body surface potential maps as templates in localizing sites of ectopic activation for radiofrequency ablation," *Physiologic Meas.*, vol. 18, pp. 373–400, 1997.

[11] R. N. W. Hauer, R. M. Heethaar, M. T. W. de Zwart, R. N. van Dijk, I. van der Tweel, C. Borst, and E. O. Robles de Medina, "Endocardial catheter mapping: Validation of a cineradiographic method for accurate localization of left ventricular sites," *Circulation*, vol. 74, no. 4, pp. 862–868, Oct. 1986.

[12] R. N. W. Hauer, M. T. de Zwart, J. M. T. de Bakker, J. F. Hitchcock, O. C. K. M. Penn, M. Nijsen-Karelse, and E. O. Robles de Medina, "Endocardial catheter mapping: Wire skeleton technique for representation of computed arrhythmogenic sites compared with intraoperative mapping," *Circulation*, vol. 74, no. 6, pp. 1346–1354, Dec. 1986.

[13] C. A. Grimbergen, A. C. MettingVanRijn, A. P. Kuiper, A. C. Linnenbank, and A. Peper, "Instrumentation for the recording and digital processing of multichannel ECG data," in *Proc. 14th Annu. Int. Conf. IEEE EMBS*, 1992, pp. 726–727.

[14] A. C. MettingVanRijn, A. P. Kuiper, A. C. Linnenbank, and C. A. Grimbergen, "Patient isolation in multichannel bioelectric recordings by digital transmission through a single optical fiber," *IEEE Trans. Biomed. Eng.*, vol. 40, pp. 302–308, Mar. 1993.

[15] A. SippensGroenewegen, H. Spekhorst, R. N. W. Hauer, N. M. van Hemel, P. Broekhuijsen, and A. J. Dunning, "A radiotransparent carbon electrode array for body surface mapping during cardiac catheterization," in *Proc. 9th Annu. Conf. IEEE EMBS*, Nov. 1987, pp. 178–181.

[16] R. L. Lux, M. J. Burgess, R. F. Wyatt, A. K. Evans, G. M. Vincent, and J. A. Abildskov, "Clinically practical lead systems for improved electrocardiography: Comparison with precordial grids and conventional lead systems," *Circulation*, vol. 59, pp. 356–363, 1979.
[17] A. C. Linnenbank, "On-site recording, analysis, and presentation of multichannel ECG data," Ph.D. dissertation, Univ. Amsterdam, Amsterdam, The Netherlands, August 1996.
[18] R. L. Lux, A. K. Evans, M. J. Burgess, R. F. Wyatt, and J. A. Abildskov, "Redundancy reduction for improved display and analysis of body surface potential maps: I. Spatial compression," *Circ. Res.*, vol. 49, pp. 186–196, 1981.
[19] B. Efron, "Estimating the error rate of a prediction rule: Improvement on cross-validation," *J. Amer. Statistical Assoc.*, vol. 78, no. 38, pp. 316–331, June 1983.
[20] R. Hren, G. Stroink, and B. M. Horáček, "Spatial resolution of body surface potential maps and magnetic field maps: A simulation study applied to the identification of ventricular pre-excitation sites," *Med. Biol. Eng. Comput.*, vol. 36, pp. 145–157, Mar. 1998.
[21] T. Kohonen, *Self-Organizing Maps*. Berlin, Germany: Springer-Verlag, 1995.
[22] J. N. Amoore, Y. Rudy, and J. Liebman, "Respiration and the ECG: A study using body surface potential maps," *J. Electrocardiol.*, vol. 21, no. 3, pp. 263–271, 1988.
[23] S. L. C. Muilwijk, "Body surface mapping of ventricular arrhythmias," Ph.D. dissertation, Univ. Amsterdam, Amsterdam, The Netherlands, 1994.
[24] S. Shpun, L. Gepstein, G. Hayam, and S. A. Ben-Haim, "Guidance of radiofrequency endocardial ablation with real-time three-dimensional magnetic navigation system," *Circulation*, vol. 96, no. 6, pp. 2016–2021, Sept. 1997.
[25] F. H. M. Wittkampf, E. F. D. Wever, R. Derksen, A. A. M. Wilde, H. Ramanna, R. N. W. Hauer, and E. O. Robles de Medina, "LocaLisa: New technique for real-time 3-dimensional localization of regular intracardiac electrodes," *Circulation*, vol. 99, pp. 1312–1317, Mar. 1999.
[26] R. A. Nadeau, P. Savard, G. Faugère, M. Shenasa, P. Pagé, R. M. Gulrajani, R. A. Guardo, and R. Cardinal, "Localization of pre-excitation sites in the Wolff-Parkinson-White syndrome by body surface potential mapping and a single moving dipole representation," in *Electrocardiographic Body Surface Mapping*, R. Th. van Dam and A. van Oosterom, Eds. Dordrecht, The Netherlands: Martinus Nijhoff, 1986, pp. 95–98.
[27] M. Dubuc, R. Nadeau, G. Tremblay, T. Kus, F. Molin, and P. Savard, "Pace mapping using body surface potential maps to guide catheter ablation of accessory pathways in patients with Wolff–Parkinson–White syndrome," *Circulation*, vol. 87, no. 1, pp. 135–143, Jan. 1993.
[28] A. SippensGroenewegen, H. A. P. Peeters, E. R. Jessurun, A. C. Linnenbank, E. O. Robles de Medina, M. D. Lesh, and N. M. van Hemel, "Body surface mapping during pacing at multiple sites in the human atrium: P-wave morphology of ectopic right atrial activation," *Circulation*, vol. 97, pp. 369–380, Feb. 1998.
[29] L. J. Leon and B. M. Horáček, "Computer model of excitation and recovery in the anisotropic myocardium: I. Rectangular and cubic arrays of excitable elements," *J. Electrocardiol.*, vol. 24, no. 1, pp. 1–15, Jan. 1991.
[30] M. Lorange and R. M. Gulrajani, "A computer heart model incorporating anisotropic propagation: I. Model construction and simulation of normal activation," *J. Electrocardiol.*, vol. 26, no. 4, pp. 245–61, Oct. 1993.
[31] Z. Xu, R. M. Gulrajani, F. Molin, M. Lorange, B. Dubé, P. Savard, and R. A. Nadeau, "A computer heart model incorporating anisotropic propagation: III. Simulation of ectopic beats," *J. Electrocardiol.*, vol. 29, no. 2, pp. 73–90, Apr. 1996.
[32] R. M. Gulrajani, *Bioelectricity and Biomagnetism*. New York: Wiley, 1998.
[33] R. Hren, G. Stroink, and B. M. Horáček, "Accuracy of single-dipole inverse solution when localizing ventricular pre-excitation sites: Simulation study," *Med. Biol. Eng. Comput.*, vol. 36, pp. 323–329, May 1998.
[34] P. Savard, A. Ackaoui, R. M. Gulrajani, R. A. Nadeau, F. A. Roberge, R. Guardo, and B. Dube, "Localization of cardiac ectopic activity in man by a single moving dipole. Comparison of different computation techniques," *J. Electrocardiol.*, vol. 18, no. 3, pp. 211–222, 1985.
[35] G. Huiskamp and F. Greensite, "A new method for myocardial activation imaging," *IEEE Trans. Biomed. Eng.*, vol. 44, pp. 433–446, June 1997.
[36] G. Huiskamp and A. van Oosterom, "The depolarization sequence of the human heart surface computed from measured body surface potentials," *IEEE Trans. Biomed. Eng.*, vol. 35, pp. 1047–1058, Dec. 1988.
[37] ——, "Tailored versus realistic geometry in the inverse problem of electrocardiography," *IEEE Trans. Biomed. Eng.*, vol. 36, pp. 827–835, Aug. 1989.

Mark Potse (S'96) received the MSc degree in physics from the University of Amsterdam, Amsterdam, The Netherlands, in 1996.

Since graduating, he has been working at the Medical Physics Department, University of Amsterdam, on a project for the real-time analysis of body surface maps supported by a grant from the Technology Foundation STW. His research interests include multichannel ECG analysis and cardiac electrophysiologic modeling.

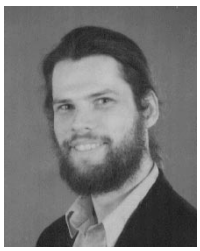

André C. Linnenbank (S'91–A'98) received the MSc degree in physics from the University of Amsterdam, Amsterdam, The Netherlands, in 1989. In 1996, he received the Ph.D. degree from the same university.

Since 1989, he has been working at the Medical Physics Department, University of Amsterdam, on a project for the real time acquisition, analysis, and presentation of body surface maps on a grant from the Technology Foundation STW. His research interests include body surface mapping, interfacing, and signal and image processing.

Heidi A. P. Peeters received the M.D. degree from the University of Leiden, Leiden, The Netherlands, in 1992. Thereafter, she joined the Department of Clinical Electrophysiology at the University Hospital Utrecht as a Clinical and Research Fellow, where she performed studies on the clinical application of body surface mapping. She received the Ph.D. degree in medicine from the University of Utrecht, Utrecht, The Netherlands, in 1997.

Since January 1998 she has been a Fellow in clinical cardiology at the University Hospital Utrecht.

Arne SippensGroenewegen received the M.D. and Ph.D. degrees in Medicine from the University of Amsterdam, Amsterdam, The Netherlands, in 1985 and 1990, respectively.

He is founder of the Dutch Body Surface Mapping Working Group. He is a Member of the Scientific Committee of the European Society of Cardiology, the International Society of Electrocardiology, the International Working Group on Body Surface Mapping, the Council on Clinical Cardiology of the American Heart Association, the Dutch Working Group on Cardiac Arrhythmias, the Dutch Society of Cardiology, and the Royal Netherlands Medical Association. After completing his training as a clinical cardiologist at the Academic Hospital of the University of Utrecht, Utrecht, The Netherlands, in 1995, he joined the Section of Cardiac Electrophysiology at the University of California at San Francisco in 1996. His research interests are in the field of clinical electrophysiology and body surface mapping.

Cornelis A. Grimbergen (M'74) received the Ir. degree in electrical engineering from the Delft University of Technology, Delft, The Netherlands. He was active in research in solid-state physics and received the Ph.D. degree from the University of Groningen, Groningen, The Netherlands, in 1977.

Since 1977, he has been with the Medical Physics Department of the University of Amsterdam, Amsterdam, The Netherlands; since 1996, as a Professor of Medical Technology. Since 1991, he has been part-time Professor of Biomedical Measuring and Control at the Control Department, Faculty of Design, Construction, and Production, Delft University of Technology. His interests are in the fields of medical instrumentation, biomedical signal and image processing, and minimally-invasive techniques.